# LEGIBILITY NOTICE

A major purpose of the Technical Information Center is to provide the broadest dissemination possible of information contained in DOE's Research and Development Reports to business, industry, the academic community, and federal, state and local governments.

Although a small portion of this report is not reproducible, it is being made available to expedite the availability of information on the research discussed herein.

1



Los Alamos National Laboratory is operated by the University of California for the United States Department of Energy under contract W-7405-ENG-36

LA-UR--90-2181

DE9 0 013118

TITLE: SHORT-RANGE NN AND N∆ CORRELATIONS IN PION DOUBLE CHARGE EXCHANGE

AUTHOR(s): MIKKEL B. JOHNSON

SUBMITTED TO: PROCEEDINGS OF THE INTERNATIONAL CONFERENCE ON MEDIUM - AND HIGH-ENERGY PHYSICS,

MAY 14-18, 1990, TAIPEI, TAIWAN, R.O.C.

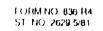
#### **DISCLAIMER**

This report was prepared as an account of work sponsored by an agency of the United States Government. Neither the United States Government nor any agency thereof, nor any of their employees, makes any warranty, express or implied, or assumes any legal liability or responsibility for the accuracy, completeness, or usefulness of any information, apparatus, product, or process disclosed, or represents that its use would not infringe privately owned rights. Reference herein to any specific commercial product, process, or service by trade name, trademark, manufacturer, or otherwise does not necessarily constitute or imply its endorsement, recommendation, or favoring by the United States Government or any agency thereof. The views and opinions of authors expressed herein do not necessarily state or reflect those of the United States Government or any agency thereof.

By acceptance of this article, the publisher recognizes that the U.S. Government retains a nonexclusive, royalty-free license to publish or reproduce the published form of this contribution, or to allow others to do so, for U.S. Government purposes.

The Los Alamos National Laboratory requests that the publisher identify this article as work performed under the auspices of the U.S. Department of Energy.







# SHORT-RANGE NN AND $N\Delta$ CORRELATIONS IN PION DOUBLE CHARGE EXCHANGE

Mikkel B. Johnson Los Alamos National Laboratory Los Alamos, New Mexico 87545, U.S.A.

I will review several important results related to the short-range nucleon-nucleon and delta-nucleon interaction that have been obtained from recent studies of pion double charge exchange in selected nuclei.

## INTRODUCTION

Pion double charge exchange (DCX) has become a unique tool for making tests of basic interactions in nuclei and for studying unusual modes of nuclear motion. What is the property of pion DCX that makes it different from other nuclear reactions? It is the fact that pion DCX occurs only if the pion interacts with at least two nucleons. In this way the pion becomes a sensitive probe of two-phonon collective modes and two-nucleon correlations, neither of which stand out in ordinary reactions because of theoretical backgrounds arising from large, dominating one-nucleon processes.

I want to discuss results of two closely related studies in this talk: the identification of the isovector delta-nucleon interaction and the signature of

short-range dynamical nucleon-nucleon correlations. Because similar dynamics underlie both phenomena, it is natural to consider the two together. Results that I will show are taken from work with numerous collaborators. The study of short-range dynamical correlations is from Ref. 1, and that concerning the delta-nucleon interaction is reviewed in Ref. 2.

Lack of time prevents me from making more than a passing mention of the measurements of two-phonon excitation that have been recently made. Examples of these include the remarkable search leading to the identification and study of the giant dipole built on the isobaric analog state, the dipole state built on the dipole, as well as the study of the isobaric analog state built on the isobaric analog state (the so-called DIAS). (See the talk by S. Mordachi at this conference.)

Before getting too deep into the talk, I should make a clear distinction between the nature of two different types of transitions that will be of interest here: double analog transitions and a special class of nonanalog transitions. One sees in Fig. 1(a) the nonanalog states that we consider. These occur in nuclei with N=Z, so each of the nucleons must change its orbit, and therefore, as a rule, its angular momentum. Furthermore, because we are dealing with scattering to the ground state, and because of the sequencing of orbits determined by the shell-model spin-orbit force, these are predominantly spin-flip transitions. Figure 1(b) shows a typical double-analog state, and one sees here that the dominant single-particle states for DIAS do not involve an orbit change of either nucleon, and thus that the nonspin-flip transitions are must important.

In this talk, I shall be concerned with the interplay between the transitions in Fig. 1 and the processes shown in Fig. 2. Figure 2(a) is sequential DCX scattering. Sequential scattering proceeds through the exchange of both  $\pi$  and  $\rho$  mesons. The rectangles represent the off-shell  $\pi N$  scattering amplitude. The term in Fig. 2(b) is the  $\Delta N$  interaction (DINT). Analogous terms, in which DCX occurs from virtual deltas in the nuclear wave function, are very small for DCX transitions to nuclear states with zero spin.<sup>3</sup> These terms, because they all involve  $\pi$  and  $\rho$  meson exchange, are particularly sensitive to short-range correlations.

Fig. 1 Depicting nonanalog and analog transitions.

Fig. 2 Processes that contribute to DCX: (a) sequential scattering, SEQ, and (b) the delta-nucleon interaction, DINT. The wiggly line represents  $\pi$ - and  $\rho$ -meson exchange.

Various backgrounds are shown in Fig. 3. Figures 3(a) and (b) show various possibilities for 6-quark structures to contribute to DCX.<sup>4</sup> Pion absorption channels may also contribute to DCX;<sup>5</sup> presumably the dominant absorption channels couple through the two-pion exchange part of the  $\Delta$ -N interaction  $V_{N\Delta}$ , but Fig. 3(c) shows another way<sup>6</sup> in which they may contribute. Finally, I show in Fig. 3(d) the possibility of DCX from the pion cloud in nuclei.<sup>7</sup>

Fig. 3 Background terms to DCX in the resonance region.

I will assume, because of the strong  $\Delta_{33}$  resonance that the processes in Fig. 3 are relatively small backgrounds to those of Fig. 2 for resonance-energy pions. The argument is harder to make at low energy, and it is of interest to ask how these mechanisms might be distinguished from one another in general. I will only remark here that I believe that such a possibility does exist, and that this possibility will be realized as the theorists evaluate the various terms and catalog their dependence on spin, isospin, and energy. This characterization will lead to an understanding of how each contributes to various elastic, single, and DCX reactions. Such a study will help to identify signatures and allow experimentalists to exploit the nucleus as a "filter" for the desired term using carefully chosen nuclear transitions. I will give an example, in the first part of my talk, of the use the sain- and energy-dependence of the processes shown in Fig. 2 to devise a filter and identify a signature for DINT. The calculations of Fig. 2 at low<sup>1</sup> and resonance energy<sup>3</sup> follow very similar patterns. We assume that the nucleons are fixed centers and apply the diagrammatic approach of Ref. 8. Corrections for nucleon and delta recoil are incorporated by making a standard frame transformation from the  $\pi N$  lab to center-of-mass (CM) system. The evaluation of the diagrams of Fig. 2 is rather tedious, but once it is accomplished, one is ready to calculate a cross section in the distorted-wave impulse approximation, taking the expectation value of  $\hat{F}_i$  for realistic shell-model wave functions and for pion distorted waves. Expressed in second-quantized form, the amplitude  $\hat{F}_i$  for each diagram takes the form

$$\widehat{F}_{i} = \frac{1}{2} \sum_{\substack{J'M'\\j_{1}j_{2}}} \sum_{\substack{JM\\j_{1}j_{2}}} (a_{j1}^{\dagger \prime} a_{j2}^{\dagger \prime})^{J'M'}$$

$$\times \langle (j'_{1}j'_{2})J'M'|D_{i}(\mathbf{k'},\mathbf{k};\mathbf{r'})\delta(\mathbf{R'}-\mathbf{R})|(j_{1}j_{2})JM\rangle (\tilde{a}_{j2}\tilde{a}_{j1})^{J-M}(-)^{-J+M}(1)$$

where  $D_i$  is the value of the diagram expressed as an operator expansion in spinisospin tensors, and  $a_j^{\dagger}$  are creation operators for nucleons of quantum numbers j (we take j to stand for a complete set of single-particle quantum numbers). The cross section is then given in terms of  $\hat{F}_i$  by  $\delta \sigma / \delta \Omega = |\sum_i \tilde{F}^i / 4\pi|^2$ , where

$$\widetilde{F}^{i}(\mathbf{k}_{0}', \mathbf{k}_{0}) = \int \chi^{\bullet(-)}(\mathbf{k}_{0}', \mathbf{R}) \\
\times \langle \psi_{Nf} | D_{i}(\mathbf{k}', \mathbf{k}; r') \delta(\mathbf{R}' - \mathbf{R}) | \psi_{Ni} \rangle \chi^{(+)}(\mathbf{k}_{0}, \mathbf{R}) d^{3}\mathbf{R} , \quad (2)$$

and where  $\chi^{\pm}$  are pion distorted waves. The expression in Eq. (2) gives the orrect way to incorporate distorted waves for DINT, because the entire DCX process takes place on the same nucleon.

For SEQ we use a modified procedure for incorporating distortions, because in this case the pion scatters from two different nucleons. One can approximately account for these differences using Eq. (2) for SEQ by simply suppressing all nuclear transitions in which the angular momentum of a single-nucleon changes. This result is consistent with coupled-channel calculations, and the reason for the suppression can be seen in the strong-absorption limit as follows. When the angular momentum of a nucleon changes, conservation of angular momentum requires that the pion change its direction. Thus, between the two charge exchanges the pion moves either outside of the nucleus where there are fewer nucleons for the second scattering, or inside the nucleus where the attenuation is strong. The pion would like to follow the optimal straight-line trajectory through the surface of the nucleus, and when it cannot do this, the cross section is suppressed.

The matrix elements of  $\hat{F}_i$  between shell-model states can be expressed in terms of  $\langle \psi_{Nf}|||\{(a_{j1'}^+,a_{j2'}^+)^{J'}(a_{j1}a_{j2})^J\}|||\psi_{Ni}\rangle$ , the two-body reduced matrix elements. For our calculations, we take these matrix elements from the shell-model program OXBASH.<sup>10</sup>

The major computational job is to evaluate the matrix elements of  $D_i$  in Eq. (1). This involves a lot of effort, especially in evaluations with Racah algebra, and I will spare you the details. We can reduce the calculation of  $D_i$  to a sum of one-dimensional integrals by performing a Moshinsky transformation from  $\mathbf{r}_1$  and  $\mathbf{r}_2$  to the relative coordinate  $\mathbf{r} = \mathbf{r}_1 - \mathbf{r}_2$  and center-of-mass coordinate  $\mathbf{R} = (\mathbf{r}_1 + \mathbf{r}_2)/2$ . The integral that we perform numerically is the one over the relative variable,

$$\int_0^\infty r^{2\prime} dr^2 R_{n'\ell'}(r') R_{n\ell}(r') H_{\alpha}(\overline{k}, r') j_{\ell}(Qr') \Gamma(r') , \qquad (3)$$

where Q is a momentum that is different for each diagram in Fig. 2. In this expression,  $\Gamma(r)$  is the two-body correlation function, which we take to be the same as the nucleon-nucleon correlation function as deduced from G-matrix calculations<sup>11</sup> to have the form

$$\Gamma(r_{12}) = 1 - j_0(q_c r_{12}) \quad , \tag{4}$$

where  $q_c = 783$  MeV/c. The function  $H_{\alpha}(\overline{k},r)$  is the propagator for a meson of momentum  $\overline{k}$  in the medium. The reaction is sensitive to  $\Gamma(r_{12})$  because  $H_{\alpha}(\overline{k},r)$  becomes large at small  $r_{12}$  for pions and rho mesons. It is important to have made the Moshinsky transformation because the short-range correlations and meson propagators act in the relative variable r, so we can focus our energies and attention on that part of the calculation where the sensitivity to short-range correlations originates.

#### THE DELTA-NUCLEON INTERACTION

The first application of pion DCX that I will discuss is scattering to nonanalog states for resonance-energy  $\pi$  scattering. I want to show how the properties

of the nucleus have been used as a filter to eliminate the large and usually dominant process of Fig. 1(a) from the piece of interest here, Fig. 1(b).

In order to calculate DINT, we need to know the coupling of a  $\pi$  and  $\rho$  meson directly to the delta 3-3 as it occurs in Fig. 1. This coupling vertex is sometimes called the double-delta vertex, and it was not known from any source when we began our work. Our model of the double-delta vertex coupling is the following, in which we have chosen the form of the matrix element to be analogous to those for the coupling of a  $\pi$  and  $\rho$  meson to the nucleon,

$$\pi \Delta \Delta : (f_{\pi \Delta \Delta}/m_{\pi}) \Sigma \cdot \mathbf{k} \Theta \cdot \hat{\pi} v_{\pi \Delta \Delta}(\mathbf{k}) , \qquad (5a)$$

$$\rho \Delta \Delta : (f_{\rho \Delta \Delta}/m_{\rho}) \Sigma \cdot \mathbf{k} \times \epsilon \Theta \cdot \hat{\rho} v_{\rho \Delta \Delta}(k) . \tag{5b}$$

We take the ratio of the pion-delta to pion-nucleon coupling constants from the  $SU(2) \times SU(2)$  quark model<sup>12</sup>  $(f_{\pi\Delta\Delta}/f_{\pi NN} = 4/5)$ , scale the  $\rho$ -to- $\pi$  coupling to the value used in the Bonn nucleon-nucleon interaction<sup>13,14</sup> with the strong  $\rho$  coupling  $(f_{\rho\Delta\Delta}/f_{\pi\Delta\Delta} = f_{\rho NN}/f_{\pi NN} = 2.6)$ , and take the mass of the  $\rho$  meson to be  $m_{\rho} = 644$  MeV in order to account for the two-pion continuum having the quantum numbers of the  $\rho$  meson.

The form factors are taken to have the following functional dependence on the momentum of the meson,

$$v_i(\mathbf{k},\omega) = (\Lambda_i^2 - m_i^2)/(\Lambda_i^2 - \mathbf{k}^2) \quad , \tag{6}$$

following the choices made in the Bonn interaction.<sup>13</sup> Here and in the following section we take the ratio of the  $\pi$  to  $\rho$  meson form factors to be the same as in the Bonn interaction,  $\Lambda_{\pi\Delta\Delta}/\Lambda_{\rho\Delta\Delta} = \Lambda_{\pi NN}/\Lambda_{\rho NN} = 6/7$ , which leaves only one parameter that is unknown, namely the  $\Lambda_{\pi\Delta\Delta}$  form-factor cutoff. In our papers (see, e.g., Ref. 3) we showed that DINT was very sensitive to the value of the double-delta form-factor cutoff, and that with reasonable choices of the cutoff, DINT can be quite large. So, there seemed to be little doubt that DINT was large enough to be seen in pion DCX. One of the main reasons for studying DINT is to make an empirical determination of the double-delta vertex coupling. The form factor is of considerable interest in its own right, because comparisons of the pion-nucleon and pion-delta form factors would make possible a conclusion

regarding the relative size of the delta and the nucleon, which is fundamental to an understanding of the strong interaction. We have adjusted  $\Lambda_{\pi\Delta\Delta}$  to fit the experimental data.

I should mention that functional dependences on the pion momenta different from ours in Eq. (6) are often assumed. For example, the cloudy-bag form factor <sup>15</sup> has the shape  $v(k) = 3j_1(kR)/(kR)$ , and the P-wave pion-nucleon form factor deduced in Ref. 16 using a Cnew-Low-inspired field-theoretical model,  $v(k) = \exp[-k^2/(2\alpha^2)]$ , with  $\alpha = 4.956 \ m_{\pi}$ . The root-mean-square (RMS) radius of the form factors is the most important common element, and we are therefore able to connect these various forms in the low-momentum limit to find

$$R^{2} = \begin{cases} 10/\Lambda^{2} & \text{Monopole} \\ 5/\alpha^{2} & \text{Exponential} \end{cases}$$
 (7)

Next, I want to discuss the signature for DINT in pion DCX. One expects a distinctive energy dependence. In particular, the DINT process in Fig. 2(b) contains two delta propagators, which means that the cross section depends on the pion energy as  $(E - m_{\Delta} + iW/2)^{-4}$ , where  $m_{\Delta}$  and W are the mass and width of the delta, respectively. This is a very strong energy variation, and we see that a rather clear signature of DINT would be a prominent bump in the cross section occurring near the delta 3-3 resonance. Distortions of the initial and final pion wave function are large in this region, so one should be prepared for some modification of the energy dependence arising from an interplay between distortions and the intrinsic energy dependence of the diagrams in Fig. 2.

What about SEQ? With regard to the energy dependence of DINT and SEQ, it is important to make the following distinctions. DINT, because it proceeds entirely through the delta, is purely P-wave. SEQ, on the other hand, has contributions from both the isovector S-wave and P-wave pion-nucleon scattering amplitude. It turns out that the isovector S-wave amplitude is large in the resonance region and interferes destructively with the P-wave amplitude below resonance and constructively with it above resonance. Consequently, when these amplitudes are considered together, SEQ tends to increase monotonically as the

pion kinetic energy is increased from 100 to 300 MeV. Thus DINT and SEQ have quite different energy dependences and can be distinguished on this basis.

The next points have to do with how one identifies an effective nuclear filter for DINT. There are two issues to be discussed, both with regard to the differences of DINT and SEQ in analog and nonanalog transitions. The first has to do with the role of distortions, and the second with the spin dependence of the mechanisms of Fig. 2.<sup>3</sup>

As we discussed earlier, the distortions strongly suppress SEQ in single-particle transitions for which the nucleon angular momentum changes. They have no such effect on DINT. Since nonanalog transitions that we are considering are dominantly of this type, this means that DINT competes with some advantage over SEQ in this case. No such suppression of SEQ occurs for DIAS transitions, and one might therefore expect that the physics of DIAS is a more equal admixture of these two processes.

The second point regards the interplay between the spin dependence of the DINT and SEQ processes and the nature of the single-particle states in analog and nonanalog transitions. One of our main results<sup>3</sup> is that the spin dependence enhances DINT relative to SEQ when the nucleon spin flips, such as in nonanalog transitions, and suppresses DINT relative to SEQ when the nucleon spin does not flip, such as in DIAS. Thus, from considerations of the spin dependence, DINT competes favorably with SEQ in nonanalog transitions. We also see from this that in DIAS transitions, DINT is perhaps suppressed relative to SEQ.

Now let us look at some data and the results of our calculations. I show first in Fig. 4 the experimental results for  $^{16}O$  compared to the theory. The solid curve is DINT normalized to the data at the peak of the cross section by an adjustment of  $\Lambda_{\pi\Delta\Delta}$ . I stress that this adjustment is the only one that is made, i.e., all results shown from this point on are predictions of the theory. The dashed curve is our calculation of SEQ calculated as explained earlier in the talk. It looks likely that the rise of the data above 250 MeV is due to the increasing importance of SEQ there. I suspect that we have somewhat overestimated our

Fig. 4 Theoretical and experimental<sup>18</sup> excitation functions for the nonanalog transition in <sup>16</sup>O.

SEQ, because our SEQ lies above the data in this high-energy region. Our results for SEQ are also larger than the results of Ref. 9. We have found SEQ to be technically difficult to calculate, and I believe that all calculations of SEQ suffer from a great deal of model dependence that will be eliminated only when corresponding single-charge-exchange data are available. For our calculations of nonanalog transitions we have simply omitted SEQ and focused our attention on the region of the peak where all calculations show SEQ to be quite suppressed. Note that the peak of DINT lies somewhat below the actual position of the 3-3 resonance, and the reason for this in our calculations is the pion distorted waves, which set in strongly as one approaches the resonance.

The form-factor cutoff  $\Lambda_{\pi\Delta\Delta} = 4.82 \text{ fm}^{-1}$  was found by fitting the theory to the data.<sup>2,17</sup> We should stress that because of the strong sensitivity of the reaction to the form-factor,<sup>3</sup> we have a very good determination of  $\Lambda$ , even though we have made some approximations elsewhere in our evaluations. This value

of  $\Lambda_{\pi\Delta\Delta}$  corresponds to a cloudy-bag radius of  $R_{\Delta} = 0.66$  fm, and this value happens to coincide closely with that determined from pion-nucleon scattering in Ref. 16 (in this case  $R_{\Delta} = 0.64$  fm<sup>-1</sup>). An approximate equality between the two values indicates a pleasing internal consistency in this analysis, which has taken elements from various other sources in nuclear physics.

Next I will show some of our results<sup>17</sup> for the delta-nucleon interaction in the remaining data sets. Figure 5 shows the energy dependence of the 5° cross section in a variety of nuclei from <sup>12</sup>C to <sup>40</sup>Ca. All the data sets show a bump, which is the expected signature of the delta-nucleon interaction. The nucleus dependence of the theory reflects the effect of the shell-model correlations, and it is

Fig. 5 Theoretical and experimental 18 excitation functions for the nonanalog transition in a variety of nuclei.

pleasing to see that the trend of the data is reproduced. Angular distributions are well reproduced by the model. The fact that the shape comes out well indicates that the interferences that seem to complicate DIAS do not occur here in the nonanalog DCX, providing additional support to our one-amplitude model for nonanalog transitions based on  $V_{\Delta N}$ .

### SHORT-RANGE DYNAMICAL CORRELATIONS IN NUCLEI

Low-energy pion double charge exchange to isobaric analog states is expected to be dominated the process shown in Fig. 2(a) for large separations between the two nucleons. To explore short-range correlations in nuclei using pion double charge exchange one needs to remove these long-range contributions. The resulting short range effects are of special interest in nuclear physics. As we have seen, they arise from the short-range repulsion that keeps nucleons apart in nuclei and the special short-range character of the pion and rho meson interactions that are quite prominent in microscopic models of the pion-nucleon interaction. 19-22 One such model of these correlations has been used already in our study of the delta-nucleon interaction. The separation between long-range and short-range can be implemented by making use of results obtained in the shell model as developed by de Shalit and Talmi.<sup>23</sup> The long-range and shortrange components of the interaction contribute differently as the number of pairs of active like particles in the nucleus is increased. In particular, for seniority zero state the general expectation value of an operator can be expressed in the following form:

$$\langle j^n, J = 0^+ | \sum_{ij} \theta_{ij} | j^n, J = 0^+ \rangle = \frac{1}{2} n(n-1)\alpha + \frac{1}{2} n\beta$$
, (8)

where the coefficient  $\alpha$  contributes for long-range interactions and the coefficient  $\beta$  contributes for zero-range (or spin-dependent) interactions. The same formalism applies to pion DCX,<sup>24,25</sup> and Weinfeld et al.<sup>26</sup> have shown using the results of Refs. 24 and 25 that this expression explains a large amount of experimental data and have extracted from the data two complex parameters A and B related to the  $\alpha$  and  $\beta$  of Eq. (8). Siciliano, Sarafian, and I have recently looked at the implications for a specific model of short-range correlations<sup>1</sup> involving pion

plus rho-meson exchange with a standard g-matrix type correlation function. I want to show the results of the latter investigation here and compare to the phenomenological work of Ref. 26.

We will show the significance of the dynamical short-range correlations for DCX scattering from the Ca isotopes, where data for several nuclei can be brought to bear on the issues.<sup>26</sup> Because we are working at low energy where the nucleus is relatively transparent, we neglect the distortions and examine relative cross sections for sensitivity to dynamical short-range correlations. For Fig. 2(a), we express the on-shell part of this amplitude in terms of empirical s-and p-wave  $\pi N$  phase shifts.<sup>27</sup> We take the form factors of the  $\pi N$  scattering amplitude from Chew-Low inspired models,<sup>16</sup> from which we deduce  $\Lambda_s = 2.1$  fm<sup>-1</sup> and  $\Lambda_p = 4.95$  fm<sup>-1</sup>.<sup>1</sup> Different functional forms, as well as values of  $\Lambda_p$ , are found in the literature. Our monopole form is the same as that of the Bonn group,<sup>13</sup> but they utilize a larger value of  $\Lambda_p$ , about 6 fm<sup>-1</sup>; Bleszynski and Glauber<sup>28,29</sup> use  $\Lambda_p = 3.5$  fm<sup>-1</sup>, and Gibbs et al.<sup>25,30</sup> use  $\Lambda_p = 1.5$  fm<sup>-1</sup>.

A similar calculation may be made for the LLEE parameter  $\xi/3$ , which has been inferred from various data to be  $0.4 \pm 0.13$ . Details of this calculation are given in Refs. 1 and 31. Including the effect of Pauli correlations, and using the same short-range correlations,  $\rho$  meson, and DINT as for our DCX, we find  $\xi/3 = 0.4$ , 0.34, and 0.16 for  $\Lambda_{\pi} = 6.08 \text{ fm}^{-1}$ , 4.95 fm<sup>-1</sup>, and 2 fm<sup>-1</sup>, respectively. Values of  $\Lambda_{\pi}$  from about 4.95 to 6 fm<sup>-1</sup> give acceptable values of the empirical LLEE parameter, but values as small as 2 fm<sup>-1</sup> yield  $\xi$  that are too small.

With  $\Gamma(r_{12})$  given in Eq. (4) the two-particle distribution function in our DCX model is changed significantly from that obtained in the pure shell-model description. For example, in Ref. 29 the S-wave two-particle distribution function is peaked at  $r_{12} = 0$ . Consequently, most of the DCX cross section comes from  $r_{12}$  being less than 2 fm,<sup>29</sup> with about half occurring for separations of less than about 1 fm.<sup>30</sup> Including  $\Gamma(r_{12})$  in the relative adial integral causes the S-wave two-particle density to vanish at  $r_{12} = 0$  (where  $\Gamma = 0$ ), and the probability removed at small  $r_{12}$  is redistributed over a broader interval in the relative separation of the two particles.

To incorporate nuclear structure, we express the diagrams in second-quantized notation, as in Eq. (1). The expectation value F of the operator  $\widehat{F}$  can be calculated in terms of the reduced two-body density matrix element  $\langle \Psi_f ||| \{[a_j^+ a_j^+]^J [\tilde{a}_j \tilde{a}_j]^J \}^0 ||| \Psi_i \rangle$ , which for a  $j^n$  configuration in the seniority scheme is deduced from Ref. 25: k(j,J,n)(2j+3-n) if J=0 and k(j,J,n)(n-2)/(j-1/2) if J= even, where  $k(j,J,n)=-\{(2J+1)(n+3)!/[6(2j+1)^2(n-1)(n-1)!]^{1/2}$ . If J= odd, the reduced matrix element is zero. In the case of  ${}^{42}\mathrm{Ca}\ (n=2)$ ,  $\widehat{F}$  receives a contribution from  $D_i$  only for J=0, whereas in  ${}^{44}\mathrm{Ca}$  and  ${}^{48}\mathrm{Ca}$ , the matrix elements with J=2,4, and 6 also enter the calculation. The intereference among these matrix elements as n=1 is varied provides the capability of separating the long- and short-range contributions to DCX and therefore the possibility of finding a distinctive signature of short-range correlations.

With the valence neutrons in Ca described by the  $j^n$  seniority scheme, Eq. (1) implies a simple scaling formula<sup>24</sup>

$$F = [n(n-1)/2]^{1/2} [\alpha + \beta/(n-1)] , \qquad (9)$$

where  $\alpha$  and  $\beta$  are two functions of angle that are independent of the number n of valence neutrons occupying the  $f_{7/2}$  shell. As long as we adopt this scheme, the same form of the scattering amplitude obtains, even when we include our short-range dynamical correlations; only the numerical values of the parameters associated with the form are affected. The relationship between the parameters A and B of Ref. 25 and  $\alpha$  and  $\beta$  is  $A = \alpha + \beta/4$  and  $B = 3\beta/4$ . The  $\alpha, \beta$  parameterization has some advantages over A and B. One can show that any spin-dependent process (e.g., DINT) must contribute only to  $\beta$ . Furthermore, zero-range interactions contribute to  $\beta$  and not to  $\alpha$ .

We present in Table I values of  $\alpha$  and  $\beta$  for the various pieces of our model given in Fig. 2. We see from Table I that at 35 MeV the short-range repulsive correlations, the  $\rho$  meson, and DINT contribute insignificantly to  $\alpha$ . This fact is consistent with the result stated above, namely that all short-range and spin-dependent effects essentially contribute only to  $\beta$ . DINT is a relatively small

Table I. Values of  $\alpha$  and  $\beta$  for the Various Processes in Fig. 2 at  $T_{\pi}=35$  MeV. The notation  $\delta\pi(\Gamma)$ ,  $\delta\rho$ , and  $\delta(\text{DINT})$  refer, respectively, to the change in the  $\alpha$  and  $\beta$  parameters when the short-range correlation function  $\Gamma(r_{12})$ , when the  $\rho$  meson and when DINT are included, and  $\delta\equiv\delta\pi(\Gamma)+\delta\rho+\delta(\text{DINT})$ .

	$\alpha \ (\times 10^3)$		$\beta \ (\times 10^3)$	
Model	Real	Ímag	Real	İmag
$\overline{SEQ \pi (\Gamma = 1)}$	-2.04,	-1.25	5.51,	8.00
$\delta\pi(\check{\Gamma})$	-0.05,	0.01	-1.56,	-0.15
$\delta \rho$	-0.20,	-0.02	-1.08,	0.10
$\delta(DINT)$	0. ,	0.	0.49,	0.03
$\delta$ `	-0.24,	-0.01	-2.16,	-0.23
Total: SEQ $\pi$ ( $\Gamma = 1$ ) + $\delta$	-2.29,	-1.26	3.35,	7.76

contribution at 35 MeV. We further note in Table I one of our main results, namely that the short-range correlation and  $\rho$ -meson effects are coherent and significantly decrease the real part of  $\beta$ . As one knows empirically from the low-energy DCX data that a strong cancellation must occur between the  $\alpha$ -and  $\beta$ -terms in Eq. (9) as n is increased, even small changes in  $\beta$  make a big difference in the n-dependence of DCX throughout isotopic multiplets at low energy. The strong, coherent suppression of  $\beta$  that we observe in Table I is sufficiently pronounced to provide a meaningful test for dynamical short-range correlations in nuclei using DCX.

We can get a measure for the importance of correlations by comparing our results to experiment. The empirical values of A and B are given in Table II. It was found<sup>26</sup> that |B/A| and  $\cos \phi$  were only weakly dependent on angle, and we compare to our values calculated at zero degrees. We see that |B/A| and  $\cos \phi$  are very sensitive to short-range dynamical correlations. The uncorrelated  $(\Gamma = 1)$  sequential process gives a large |B/A|, but this value is more than twice that of the data. The addition of repulsive correlations and DINT decreases |B/A| by about 30%. The phase  $\phi$  is slightly worsened, but overall, the repulsive correlations lead to an improvement in the description of DCX in the Ca isotopes. Adding the  $\rho$  meson contribution leads to a further decrease of |B/A| and  $\phi$  that seems quite compatible with the experimental results.

Table II. Values of |B/A| and  $\cos \phi$  at  $T_{\pi}=35$  MeV. The model corresponds to  $\Lambda_{\pi}=4.95$  fm<sup>-1</sup>, and  $\phi$  is the relative phase of A and B.

B/A	$\cos \phi$	$\chi^2/N$
7.2	0.23	23
5.5	0.12	8
4.0	0.03	3
$3.5\pm0.8$	$0.55\pm0.3$	
	7.2 5.5 4.0	7.2 0.23 5.5 0.12 4.0 0.03

A refined calculation requires configuration mixing, which in Ref. 28 enhances the cross section for <sup>42</sup>Ca. We have found with the same prescription that the data no longer decisively favor one model over another, despite the continuing strong sensitivity to dynamical short-range correlations. Although Bleszynski and Glauper<sup>28</sup> find excellent agreement with the Ca data without including short-range correlations, I want to emphasize that this agreement does not rule out substantial dynamical short-range correlation effects. Unfortunately, until the experimental situation improves, conclusive evidence for or against dynamical short-range correlations can not emerge from these low-energy DCX measurements.

In closing, I would say that pion DCX has given us a hitherto unavailable handle on nuclear dynamics. The competing ideas for explaining the data are large in number, and the task of sorting them out is not yet finished. I have tried to give you a list of some of the more important ones and at the same time indicate the source of my optimism why, with careful investigations, signatures will be obtained for distinguishing the various possibilities.

#### ACKNOWLEDGEMENT

I would like to thank Prof. H.-Y. Hwang for his hospitality and for the invitation to this conference.

#### REFERENCES

- E. R. Siciliano, M. B. Johnson, and H. Sarafian (to appear in Ann. Phys. (NY), July 1990); M. B. Johnson, E. R. Siciliano, and H. Sarafian (to appear in Phys. Lett. B).
- 2. M. B. Johnson, in "Second LAMPF Workshop on Pion Double Charge Exchange" (to be published by World Scientific).
- M. B. Johnson, E. R. Siciliano, H. Toki, and A. Wirzba, Phys. Rev. Lett.
   52, 593 (1984); A. Wirzba, H. Toki, E. R. Siciliano, M. B. Johnson, and R. Gilman, Phys. Rev. C40, 2745 (1989).
- 4. L. Kisslinger, in "Second LAMPF Workshop on Pion Double Charge Exchange" (to be published by World Scientific).
- 5. D. Koltun, in "Second LAMPF Workshop on Pion Double Charge Exchange" (to be published by World Scientific).
- 6. C.-R. Ching, in "Second LAMPF Workshop on Pion Double Charge Exchange" (to be published by World Scientific).
- 7. E. Oset, in "Second LAMPF Workshop on Pion Double Charge Exchange" (to be published by World Scientific).
- 8. M. B. Johnson and D. J. Ernst, Phys. Rev. C27, 709 (1983).
- 9. M. Gmitro, J. Kvasil, and R. Mach, Phys. Rev. C31, 1349 (1985).
- A. Etchegoyen, W. D. M. Rae, N. S. Godwin, and B. A. Brown, Michigan State Cyclotron Laboratory report 524 (1985).
- G E. Brown, S. O. Bäckman, E. Oset, and W. Weise, Nucl. Phys. A286, 191 (1977).
- 12. G. E. Brown and W. Weise, Phys. Rep. 22, 279 (1975).
- 13. R. Machleidt, K. Holinde, and Ch. Elster, Phys. Rep. 149, 1 (1987).
- 14. T. Hippchen, J. Speth, and M. B. Johnson, Phys. Rev. C40, 1316 (1989).
- 15. S. Thèberge, A. W. Thomas, and G. A. Miller, Phys. Rev. D22, 2838 (1980).
- 16. D. J. Ernst and M. B. Johnson, Phys. Rev. C22, 651 (1980).
- 17. R. Gilman, H. T. Fortune, M. B. Johnson, E. R. Siciliano, H. Toki, A. Wirzba, and B. A. Brown, Phys. Rev. C34, 1895 (1986).
- See, e.g., R. Gilman, Ph.D. thesis, University of Pennsylvania, 1985, Los Alamos National Laboratory report LA-10524-T; or L. C. Bland, in "Proceedings of the LAMPF Workshop on Pion Double Charge Exchange," Los

- Alamos National Laboratory Report LA-10550-C, 1985, H. W. Baer and M. J. Leitch, Eds., p. 245.
- 19. W. M. Alberico, M. Ericson, and A. Molinari, Nucl. Phys. A379, 429 (1982).
- 20. A. B. Migdal, "Theory of Finite Fermi Systems and Applications to Atomic Nuclei" (John Wiley and Sons, New York, 1957).
- 21. M. Ericson and T. E. O. Ericson, Ann. Phys. (NY) 36, 323 (1966).
- 22. G. Baym and G. E. Brown, Nucl. Phys. A247, 345 (1975).
- 23. A. de Shalit and I. Talmi, "Nuclear Shell Model" (Academic Press, New York, 1963).
- N. Auerbach, W. R. Gibbs, and E. Piasetzky, Phys. Rev. Lett. 59, 1076 (1987).
- N. Auerbach, W. R. Gibbs, J. N. Ginocchio, and W. Kaufmann, Phys. Rev. C38, 1277 (1988).
- H. W. Baer et al., Phys. Rev. C35, 1425 (1987); Z. Weinfeld et al., Phys. Rev. C37, 902 (1988); Z. Weinfeld, et al., Phys. Lett. B 237, 33 (1990).
- 27. Program SAID, R. A. Arndt, Virginia Polytechnic Institute and State University, Summer 1988 (S88) solution.
- 28. E. Bleszynski, M. Bleszynski, and R. J. Glauber, Phys. Rev. Lett. 60, 1483 (1988).
- 29. M. Bleszynski and R. Glauber, Phys. Rev. C36, 681 (1987).
- W. R. Gibbs, W. B. Kaufmann, and P. B. Siegel, in "Proceedings of the LAMPF Workshop on Pion Double Charge Exchange," Los Alamos National Laboratory report LA-10550-C (1985), p. 90.
- M. B. Johnson, in "Pion-Nucleus Physics: Future Directions and New Facilities at LAMPF," R. J. Peterson and D. D. Strottman, Eds., AIP Conf. Proc. 163 (American Institute of Physics, New York, 1983) p. 352.
- 32. J. N. Ginocchio, Phys. Rev. C40, 2168 (1989).